

Fractional Amplitude of Low-Frequency Fluctuations and Regional Homogeneity Analyses Revealed Altered Local Spontaneous Neural Activities in Ankylosing Spondylitis

Churong Lin^{1,*}, Ya Xie^{2,*}, Dong Liu², Budian Liu², Jieruo Gu², Xiaohong Wang¹, Jie Qin¹

¹Radiology Department, The Third Affiliated Hospital of Sun Yat-sen University, Guangzhou, People's Republic of China; ²Department of Rheumatology and Immunology, The Third Affiliated Hospital of Sun Yat-Sen University, Guangzhou, People's Republic of China

*These authors contributed equally to this work

Correspondence: Xiaohong Wang; Jie Qin, The Third Affiliated Hospital of Sun Yat-sen University, 600 Tianhe Road, Tianhe District, Guangzhou, Guangdong, People's Republic of China, Email wxhcrz@163.com; qinjie@mail.sysu.edu.cn

Purpose: Previous studies have revealed alterations of the functional connectivity of the brain networks in ankylosing spondylitis (AS). Fractional amplitude of low-frequency fluctuations (fALFF) and regional homogeneity (ReHo) are both voxel-based functional metrics capable of estimating local spontaneous neural activities. This study aimed to investigate the local spontaneous neural activities in AS patients by utilizing the analytical approaches of fALFF and ReHo.

Patients and Methods: A total of 78 AS patients and 59 healthy controls (HCs) underwent resting-state functional magnetic resonance imaging. fALFF and ReHo maps were generated to identify brain regions with aberrations of spontaneous neural activities in AS patients. Different frequency bands, including the standard frequency band (0.01–0.1 Hz), slow-5 (0.01–0.027 Hz), and slow-4 (0.027–0.073 Hz), were adopted in the fALFF analysis.

Results: Compared with HCs, AS patients exhibited extensive alterations of fALFF and ReHo values in brain regions belonging to the default mode network (DMN), salience network (SN), frontoparietal network (FPN), sensorimotor network, visual network and the cerebellum. Clusters found in the slow-5 band only showed significantly decreased fALFF values, whereas the slow-4 was the major contributor to the elevated fALFF values in the standard band.

Conclusion: The fALFF and ReHo analyses consistently revealed significantly altered local spontaneous neural activities in AS patients, especially in the DMN, SN and FPN, comprising the triple network model. The slow-4 band might be more sensitive to the elevated fALFF values in AS patients than the slow-5 band. Our findings provide further evidence that the aberrations of the triple network model serve as an important feature of AS from the perspective of local neural activities.

Keywords: functional magnetic resonance imaging, ankylosing spondylitis, low-frequency oscillations, brain network

Introduction

Ankylosing spondylitis (AS) belongs to a group of diseases known as inflammatory arthropathies, often characterized by inflammation and subsequent structural changes in the axial skeleton, notably the sacroiliac joint and the spine.^{1,2} The most significant clinical manifestation of AS is inflammatory back pain (IBP), characterized by insidious onset of lower back pain, which could be aggravated by rest and alleviated by activity, often accompanied by morning stiffness.³ Apart from IBP, AS patients could also present with peripheral arthritis, enthesitis and dactylitis, all of which compose the disease burden of pain in AS patients.³

It has been reported that nociceptive, neuropathic and nociplastic mechanisms all participate in the perception of pain in AS patients.^{4–6} An important tool for investigating the neural mechanism of pain perception and identifying the

functional brain abnormalities in diseases is functional magnetic resonance imaging (fMRI). Compared with the conventional task-based schemes, resting-state functional MRI (rs-fMRI) provides an opportunity to analyze the spontaneous fluctuations of the blood oxygenation level dependent (BOLD) signals while placing the patients in a wakeful rest.⁷ Several neuroimaging studies have utilized rs-fMRI to investigate the resting-state functional connectivity of different brain areas in AS. Hemington et al conducted seed-based correlation analysis (SCA) on the rs-fMRI data of 20 AS patients, and concluded that AS patients demonstrated less anti-correlated functional connectivity between the salience network and the default mode network.⁸ Liu et al utilized the graph-theory based analysis and showed that there were functional abnormalities distributed in the default mode network (DMN), salience network (SN), sensori-motor network, dorsal attention network and task control network.⁹ Another neuroimaging study utilizing independent component analysis (ICA) revealed that in comparison to AS, patients with fibromyalgia exhibited significantly decreased functional connectivity between the dorsal default mode network and the left caudate nucleus, suggesting aberrations of the cortico-striato-thalamo-cortical circuits in FM.¹⁰

While SCA, ICA and graph-theory based analysis mostly focus on the temporal synchrony and global integration of brain regions and large-scale brain networks, there are also analytical approaches dedicated to the investigation of local spontaneous neural activities. The amplitude of low frequency fluctuations (ALFF) assesses the amplitude of spontaneous neural activities by calculating the square root of the power spectrum, while the fractional amplitude of low-frequency fluctuation (fALFF) calculates the relative contribution of low-frequency fluctuations within a specific frequency band to the whole spectrum.¹¹ Compared with ALFF, fALFF is less likely to be impacted by the movement artifacts, and it is also less susceptible to physiologic noise such as respiration.^{11,12} The full power spectrum is generally divided into four frequency bands: slow-5 band (0.01–0.027Hz), slow-4 band (0.027–0.073Hz), slow-3 band (0.073–0.198Hz) and slow-2 band (0.198–0.25Hz).^{12,13} Li et al investigated the differences of ALFF between AS patients and healthy controls, and found significantly higher ALFF in brain regions such as left cerebellum anterior lobe and left postcentral gyrus, as well as lower ALFF in brain regions such as left medial frontal gyrus and right precentral gyrus.¹⁴ Rogachov et al further conducted sub-band analysis on the low-frequency oscillations (LFOs) in AS patients, showing that the slow-5 alterations were restricted to the ascending pain pathway (thalamus and S1), while the slow-4 alterations also included DMN and SN.¹⁵ The elevated LFOs within the thalamus and S1 indicated increased sensory traffic that could be construed as ongoing, fluctuating pain input, which might be specific to a certain frequency (slow-5 to slow-4 border).¹⁶ On the other hand, altered slow-4 LFOs within DMN and SN could be attributed to the pain-related rumination and negative internal thoughts. Apart from ALFF and fALFF, regional homogeneity (ReHo) is also an indicator reflecting the local synchrony and coordination, calculated as the Kendall's coefficient concordance (KCC, a statistic measuring multivariate consistency) between the time series of the local voxel and its adjacent voxels.¹⁷ To the best of our knowledge, no study has employed the analytical approach of ReHo in AS patients.

This study aimed to investigate the alterations of the regional spontaneous neural activities in AS patients by employing the analytical approaches of fALFF and ReHo, and to calculate their correlation with the clinical traits of AS patients, such as the pain scale and fatigue severity scale. Moreover, sub-band analysis of fALFF was applied to investigate whether such alterations were restricted to a certain frequency. This study hypothesized that patients with AS might present aberrant local spontaneous neural activities in certain brain areas, likely elevated fALFF and ReHo values within the pain pathways and large-scale brain networks such as sensori-motor network, DMN, SN, which could be correlated with clinical measures such as pain levels or disease activity in patients with AS. By examining the local neural activities, we could complement our understanding of the neuropathophysiological mechanisms of pain perception in patients with AS.

Methods

Participants

A total of 88 AS patients and 64 healthy controls (HCs) were recruited from the outpatient rheumatology clinic of the Third Affiliated Hospital of Sun Yat-sen University. The AS patients and the HCs were age-matched. Three AS patients

and two HCs were excluded due to excessive head motion, while three AS patients and one HC were excluded due to missing volumes or having different scanning protocols. Four AS patients and three HCs were excluded from the formal analysis due to unsatisfactory image quality during the quality control process. The inclusion criteria for the AS cohort were as follows: 1) fulfilling the 1984 Modified New York Criteria for the diagnosis of ankylosing spondylitis;¹⁸ 2) overall back pain score ≥ 1 (on a 0–10 scale) in the past 3 months; 3) no history of biologic disease-modifying anti-rheumatic drugs (bDMARDs) over the past two months, including TNF- α inhibitors and IL-17 inhibitors. Exclusion criteria were as follows: 1) contraindications for MRI, including claustrophobia and medical implants incompatible with MRI; 2) a history of psychiatric, neurologic, or metabolic conditions; 3) serious infection resulting in hospitalization or intravenous antibiotics in the past 2 months. Patients of the AS cohort were allowed to remain on stable preventative or as-needed medication (non-steroidal anti-inflammatory drugs, NSAIDs). The exclusion criteria for the HCs were as follows: 1) present conditions associated with pain, such as migraine, fibromyalgia or lumbar disc herniation; 2) having taken any analgesic medication other than NSAIDs within one month of the MRI scan or for more than a month within the last 6 months.

This study was approved by the Research Ethics Board of the Third Affiliated Hospital of Sun Yat-sen University. Written informed consent was obtained from all patients prior to inclusion in this study according to the Declaration of Helsinki.

Clinical Assessment

Age and sex of each participant were recorded at the time of the inclusion. For each AS patient, the disease duration, current pain at the time of the scan and global pain in the past week were recorded. Pain levels were assessed using the visual analogue scale (0 = no pain, 1 = pain threshold, 10 = worst bearable pain). The Fatigue Severity Scale, which is a 9-item, 7-point scale, was utilized to assess the extent of fatigue in AS patients.¹⁹ Disease activity was assessed using Bath Ankylosing Spondylitis Disease Activity Index (BASDAI).²⁰ Laboratory results including HLA-B27 positivity, C-reactive protein (CRP) and erythrocyte sedimentation rate (ESR) were also recorded.

Neuroimaging Acquisition

Magnetic resonance imaging (MRI) of the brain was conducted on all subjects using a 3.0-Tesla MR system (Discovery MR750, General Electric, Milwaukee, WI), along with an 8-channel phased-array head coil. Each participant was asked to lie still in the supine position with their eyes open and to avoid falling asleep. To minimize head movement, foam padding was placed around the exterior of the head. Structural and functional MRI data were acquired during a single scanning session. Structural (3D T1-weighted) MRI data were acquired using a 3D BRAVO sequence (flip angle = 9, TR = 6.6 ms, TE = 2.5 ms, matrix size = 256 \times 256, slice thickness = 1 mm, number of slices = 176, time of acquisition: 3:50 min). Resting-state fMRI data were acquired using a blood oxygenation level-dependent (BOLD) protocol with a T2*-weighted gradient echo planar imaging (EPI) sequence (flip angle = 90, TR = 2000 ms, TE = 30 ms, matrix size = 192 \times 192, slice thickness = 3 mm, number of slices = 41, 240 dynamics, time of acquisition = 8 min). All images were carefully inspected for quality by a rheumatologist and a radiologist.

fMRI Data Preprocessing and Analysis

fMRI Data Preprocessing

The fMRI data preprocessing was performed in the toolbox for the Data Processing and Analysis for (Resting state) Brain Imaging (DPABI v8.2).²¹ The first 10 volumes of the fMRI scans were removed for the purpose of signal stabilization. We used the orient/QC module in the DPARBI pipeline to adjust the orientation of the images and visually verify the image quality. The images were rated on a 1–5 scale, and the threshold of the QC score was set at 3. Images with QC scores < 3 were considered of poor quality and were excluded from further analysis. This was followed by slice-timing, realignment and detrending. Head motion correction was performed using the Friston 24-parameter model.²² Nuisance covariates were regressed out, including white matter signals, cerebrospinal fluid signals and the global mean signals. The images were normalized to the MNI space using T1 images and then smoothed with a Gaussian kernel of 4 mm full width at half maximum (FWHM) only for fALFF analysis. Band-pass filtering with 0.01–0.1 Hz was conducted

only for the ReHo analysis to reduce the effects of low-frequency drift and high-frequency physiological noise. Head motion was quantified as the mean framewise displacement (FD) Jenkinson values.²³ Participants with a mean FD Jenkinson value >0.2 mm were considered as subjects with excessive head motion and thereby excluded from this study.

Calculation of fALFF and ReHo

The toolbox of Data Processing Assistant for resting-state fMRI (DPARSF) from DPABI v8.2 was employed to calculate the whole-brain fALFF and ReHo values.²⁴ For fALFF analysis, fast Fourier transforms were conducted, followed by the calculation of the average square root of the power spectrum. The fALFF values were calculated as the ratio of the power spectrum of the selected frequency range to the full power spectrum.¹¹ The frequency range of the standard fALFF values was 0.01–0.1 Hz, while the slow-5 and slow-4 band were 0.01–0.027 Hz and 0.027–0.073 Hz, respectively. We also used Fisher *r*-to-*z* transformation to improve the normality of the fALFF values. For ReHo analysis, the ReHo map of each participant was generated by calculating the Kendall's coefficient concordance of the time series of a given voxel with the time series with its neighboring voxels (26 voxels) in a voxel-wise manner.¹⁷ The ReHo maps were standardized to ReHo *z*-values by subtracting the mean ReHo value of the whole brain from each voxel and divide it by the standard deviation.

Statistical Analysis

Demographic and Clinical Characteristics

Statistical analyses of the demographic and clinical characteristics were conducted using the R platform (R version 4.4.1). For categorical variables, the chi-square test was used for group comparison. For continuous variables, we first conducted the Shapiro–Wilk test to determine whether the data conformed to normal distribution. If normal distribution was fulfilled, the mean value with the standard deviation was presented, and a two-sample *t*-test was applied to compare the differences between AS patients and HCs; if not, the median with the interquartile range was presented, and the Mann–Whitney *U*-test was applied to detect group differences.

fALFF and ReHo Analysis

Two-sample *T*-test was performed in the analysis of both fALFF and ReHo, correcting for age, sex and mean FD Jenkinson value for each participant. To improve the reliability of the results, we ran voxel-wise permutation tests with 5,000 permutations using threshold-free cluster enhancement (TFCE, a nonparametric method for cluster-level inference). The significance level was set at a cluster-level Family Wise Error (FWE)-corrected $p < 0.05$ (with TFCE) and a cluster size >100 voxels. Masks were generated based on the clusters of fALFF and ReHo group comparisons, and the average fALFF and ReHo values within each cluster were extracted from each participant using the masks. Pearson correlation analyses were conducted between the extracted fALFF values as well as the ReHo values and the current VAS, global pain, BASDAI, disease duration, FSS, and CRP of the participants. Since a total of six parameters were used in the correlation analysis, a *p*-value of $0.05/6=0.0083$ was considered significant.

Results

Descriptive Statistics

The demographic and clinical characteristics of the participants are summarized in [Table 1](#). The age and sex were comparable between the HCs and AS patients ($p = 0.88$ and $p = 0.41$, respectively). Disease duration, current clinical pain, total back pain and CRP level did not conform to a normal distribution (all $p < 0.05$). Therefore, the median and the interquartile range of these variables are presented. 61.5% of the AS patients were currently or previously on NSAIDs medication, whereas 37.1% of the AS patients had a history of bDMARDs medication.

fALFF Analysis

In the standard frequency band (0.01–0.1 Hz), three clusters showed significantly increased fALFF values in AS patients, whereas one cluster showed significantly decreased fALFF values. ([Figure 1A](#)) Clusters with significantly increased fALFF values were located at the bilateral precentral gyrus and postcentral gyrus, bilateral superior parietal lobule, bilateral cuneus,

Table 1 Demographic and Clinical Characteristics of the Participants of This Study

| | AS (n=78) | HCs (n=59) | P-value |
|---------------------------------|---------------|------------|---------|
| Age (years) | 31.78±10.14 | 31.54±7.45 | 0.88 |
| Male/female | 54/24 | 36/23 | 0.41 |
| Disease duration (years) | 5[2–11.25] | / | / |
| Current VAS (0–10) | 3[2–5.5] | / | / |
| Total back pain (0–10) | 5[2.5–6] | / | / |
| FSS | 3.96±2.54 | / | / |
| BASDAI | 3.30±1.85 | / | / |
| CRP (mg/L) | 6.6[1.3–26.8] | / | / |
| HLA-B27 positivity | 70/78(89.7%) | / | / |
| Medication | | | |
| NSAIDs | 48/78(61.5%) | / | / |
| bDMARDs* | 29/78(37.1%) | / | / |
| Corticosteroids | 1/78(1.3%) | / | / |

Note: *Representative of previous bDMARDs use.

Abbreviations: AS, ankylosing spondylitis; HCs, healthy controls; VAS, visual analog scale; FSS, fatigue severity scale; BASDAI, Bath Ankylosing Spondylitis Disease Activity Index; CRP, C-reactive protein; NSAIDs, nonsteroidal anti-inflammatory drugs; bDMARDs, biological disease-modifying antirheumatic drugs.

right precuneus (Cluster 1), right insular cortex (Cluster 2), and right middle temporal gyrus (MTG; Cluster 3). One cluster located at the bilateral posterior lobe of the cerebellum exhibited significantly decreased fALFF values in AS patients in comparison to HCs.

In the slow-5 band, all three clusters showed significantly decreased fALFF values in AS patients (Figure 1B). The three clusters were identified as the bilateral posterior lobe of the cerebellum (Cluster 1), the right insular cortex (Cluster 2), and the anterior cingulate cortex (ACC) extending to the corpus callosum (Cluster 3). We could not identify any clusters with significantly increased fALFF values compared with HCs.

In the slow-4 band, we found two clusters with significantly increased fALFF values, and one cluster with significantly decreased fALFF values. (Figure 1C) The clusters with significantly increased fALFF values were located at the bilateral precentral gyrus and post-central gyrus as well as the bilateral superior parietal lobule (Cluster 1), the cuneus and the right precuneus (Cluster 2). The bilateral posterior lobe of the cerebellum also exhibited significantly decreased fALFF values in AS patients in the slow-4 band (Cluster 3).

The characteristics of the significant clusters found in the three frequency bands are summarized in Table 2.

ReHo Analysis

In the ReHo analysis, we identified five clusters with significantly increased ReHo values and two clusters with significantly decreased ReHo values in AS patients in comparison with HCs. (Figure 2) Brain regions that showed significantly increased ReHo values were identified as the bilateral precentral gyrus, postcentral gyrus, superior parietal lobule (Cluster 1 and 2), bilateral cuneus, right precuneus, and the anterior lobe of the cerebellum (Cluster 3), right MTG (Cluster 4), and the right insular cortex extending to the adjacent white matter (Cluster 5).

The brain regions with significantly decreased ReHo values were located at the bilateral posterior lobe of the cerebellum (Cluster 6), and the bilateral medial prefrontal cortex (mPFC), the anterior cingulate cortex (ACC), and bilateral dorsolateral prefrontal cortex (dlPFC; Cluster 7).

The characteristics of the significant clusters found in the ReHo analysis are summarized in Table 3.

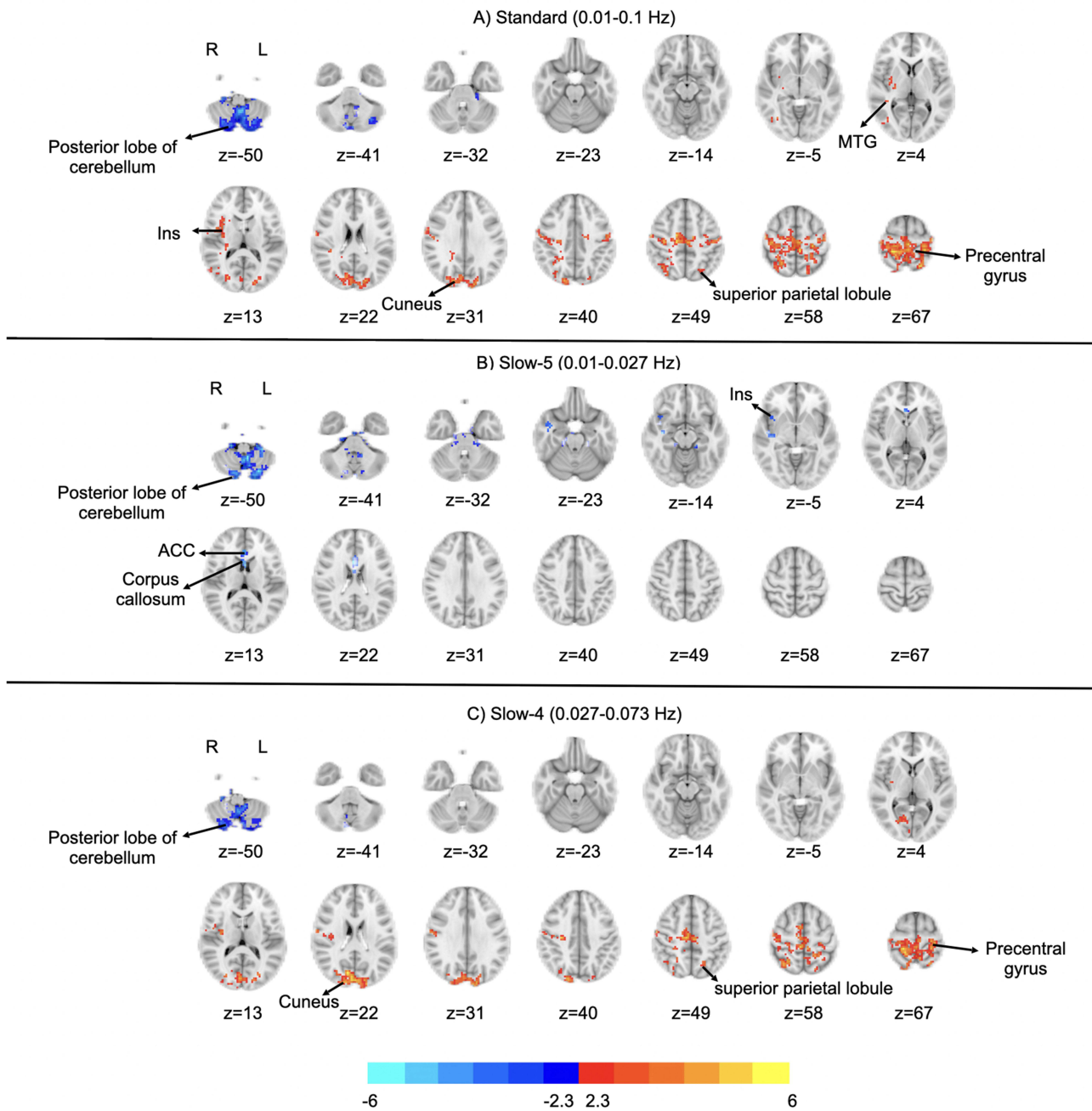


Figure 1 Regions with significantly altered fALFF values in AS patients in comparison with HCs in different frequency bands, controlling for age, sex and head motion. **(A)** Regions with significantly altered fALFF values in the standard frequency band (0.01–0.1Hz). **(B)** Regions with significantly altered fALFF values in the slow-5 band (0.01–0.027Hz). **(C)** Regions with significantly altered fALFF values in the slow-4 band (0.027–0.073Hz). Regions are presented on MNI standard brain, showing regions with z value > 2.3. Blue indicates regions with significantly decreased fALFF values, while red indicates regions with significantly increased fALFF values.

Abbreviations: fALFF, fractional amplitude of low-frequency fluctuations; AS, ankylosing spondylitis; HCs, healthy controls; MNI, Montreal Neurological Institute; L, left; R, right; MTG, middle temporal gyrus; Ins, insular cortex; ACC, anterior cingulate cortex.

Pearson Correlation Analysis

Results of the Pearson correlation analysis are presented in [Supplementary Figure S1-S17](#). Only the ReHo values in the precentral and postcentral gyri were negatively correlated with the FSS ($r = -0.36$, $p = 0.0013$, [Figure 3](#)). No significant correlation was found between the fALFF values in the standard frequency band, slow-5 band or slow-4 band and the clinical characteristics.

Table 2 Clusters with Significantly Altered fALFF Values in AS Patients in Comparison with HCs Identified in the fALFF Analysis, Including the Standard Frequency Band (0.01–0.1Hz), Slow-5 Band (0.01–0.027Hz) and Slow-4 Band (0.027–0.073Hz)

| Cluster | Contrast | Number of Voxels | MNI Coordinates | | | Peak Intensity | Brain Regions |
|--------------------------------|----------|------------------|-----------------|-----|-----|----------------|---|
| | | | X | Y | Z | | |
| Standard (0.01–0.1 Hz) | | | | | | | |
| Cluster 1 | AS>HCs | 2640 | 42 | -21 | 60 | 5.360 | Bilateral precentral gyrus and post-central gyrus, bilateral superior parietal lobule, bilateral cuneus and right precuneus |
| Cluster 2 | AS>HCs | 174 | 33 | 0 | -3 | 4.522 | Right insular cortex |
| Cluster 3 | AS>HCs | 108 | 48 | -75 | 6 | 3.870 | Right MTG |
| Cluster 4 | AS<HCs | 1046 | 0 | -57 | -54 | -6.086 | Bilateral posterior lobe of the cerebellum |
| Slow 5 (0.01–0.027 Hz) | | | | | | | |
| Cluster 1 | AS<HCs | 1206 | -21 | -81 | -54 | -4.939 | Bilateral posterior lobe of the cerebellum |
| Cluster 2 | AS<HCs | 114 | 39 | -18 | -12 | -4.233 | Right insular cortex |
| Cluster 3 | AS<HCs | 145 | 3 | 15 | 21 | -4.643 | Anterior cingulate cortex extending to the corpus callosum |
| Slow 4 (0.027–0.073 Hz) | | | | | | | |
| Cluster 1 | AS>HCs | 1531 | 21 | -36 | 63 | 5.130 | Bilateral precentral gyrus and post-central gyrus, bilateral superior parietal lobule |
| Cluster 2 | AS>HCs | 705 | -12 | -96 | 27 | 5.035 | Cuneus and right precuneus |
| Cluster 3 | AS<HCs | 806 | 0 | -57 | -54 | -6.114 | Bilateral posterior lobe of the cerebellum |

Notes: The X, Y, Z represent the peak MNI coordinates.

Abbreviations: fALFF, fractional amplitude of low-frequency fluctuations; AS, ankylosing spondylitis; HCs, healthy controls; MNI, Montreal Neurological Institute; MTG, middle temporal gyrus.

Discussion

This is the first study to examine the spontaneous neural activities by employing the analytical approaches of fALFF and ReHo in AS patients with chronic lower back pain. In addition to the standard frequency band of fALFF, we also studied

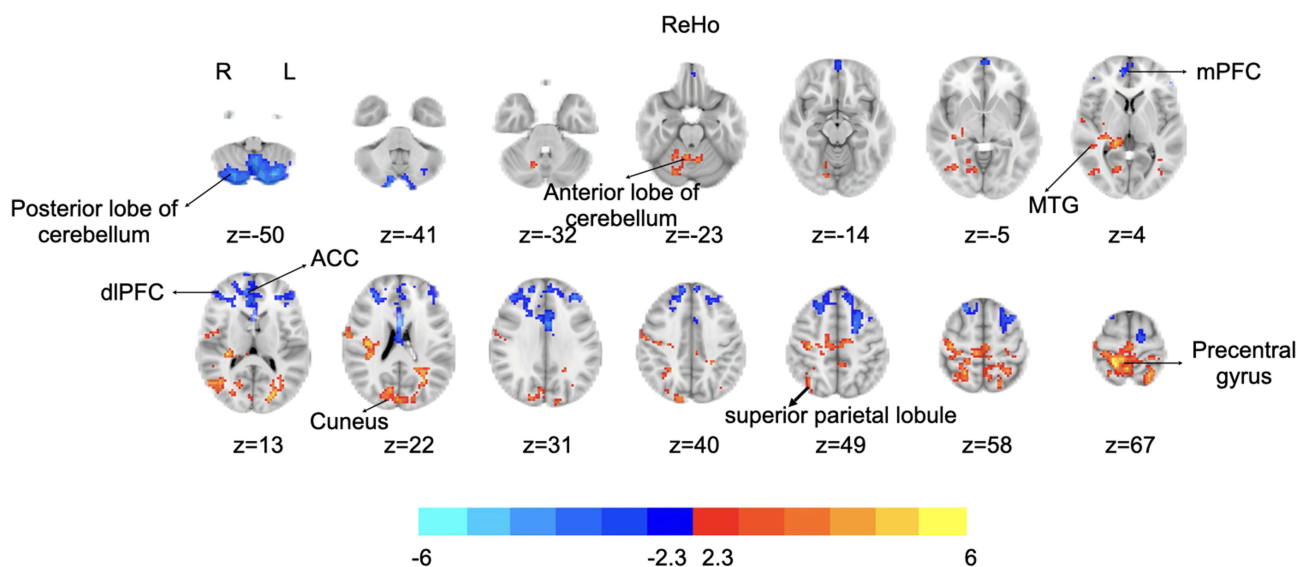


Figure 2 Regions with significantly altered ReHo values in AS patients in comparison with HCs, controlling for age, sex and head motion. Regions are presented on MNI standard brain, showing regions with z value > 2.3. Blue indicates regions with significantly decreased ReHo values, while red indicates regions with significantly increased ReHo values.

Abbreviations: ReHo, regional homogeneity; AS, ankylosing spondylitis; HCs, healthy controls; MNI, Montreal Neurological Institute; L, left; R, right; MTG, middle temporal gyrus; mPFC, medial prefrontal cortex; ACC, anterior cingulate cortex; dIPFC, dorsolateral prefrontal cortex.

Table 3 Clusters with Significantly Altered ReHo Values in AS Patients in Comparison with HCs Identified in the ReHo Analysis

| Cluster | Contrast | Number of Voxels | MNI Coordinate | | | Peak Intensity | Structures Involved |
|-----------|----------|------------------|----------------|-----|-----|----------------|---|
| | | | X | Y | Z | | |
| Cluster 1 | AS>HCs | 119 | 63 | -6 | 21 | 3.6389 | Bilateral precentral gyrus and postcentral gyrus, superior parietal lobule |
| Cluster 2 | AS>HCs | 1296 | 18 | -42 | 63 | 5.0827 | |
| Cluster 3 | AS>HCs | 778 | -21 | -81 | 15 | 4.7516 | Bilateral cuneus and right precuneus as well as the anterior lobe of the cerebellum |
| Cluster 4 | AS>HCs | 144 | 51 | -75 | 9 | 4.5675 | Right MTG |
| Cluster 5 | AS>HCs | 286 | 27 | -30 | 0 | 4.9104 | Right insular cortex extending to the adjacent white matter |
| Cluster 6 | AS<HCs | 992 | -9 | -78 | -54 | -5.2574 | Bilateral posterior lobe of the cerebellum |
| Cluster 7 | AS<HCs | 1791 | 0 | 12 | 18 | -5.6521 | Bilateral mPFC, ACC, and bilateral dIPFC |

Notes: The X, Y, Z represent the peak MNI coordinates.

Abbreviations: ReHo, regional homogeneity; AS, ankylosing spondylitis; HCs, healthy controls; MNI, Montreal Neurological Institute; MTG, middle temporal gyrus; mPFC, medial prefrontal cortex; ACC, anterior cingulate cortex; dIPFC, dorsolateral prefrontal cortex.

the contribution of both the slow-5 and slow-4 bands to the alterations of the standard frequency band. The main result of this study was that the fALFF and ReHo analyses consistently revealed aberrantly increased spontaneous neural activities in the bilateral precentral and postcentral gyri, bilateral cuneus, right precuneus, right MTG, and right insular cortex, while the spontaneous neural activities in the bilateral posterior lobe of the cerebellum were aberrantly decreased. Moreover, ReHo analysis revealed significantly increased ReHo values in the bilateral anterior lobe of the cerebellum, and significantly decreased ReHo values in the bilateral mPFC, ACC, and bilateral dIPFC, all belonging to the triple network model, including the default mode network, salience network, and frontoparietal network (FPN).²⁵

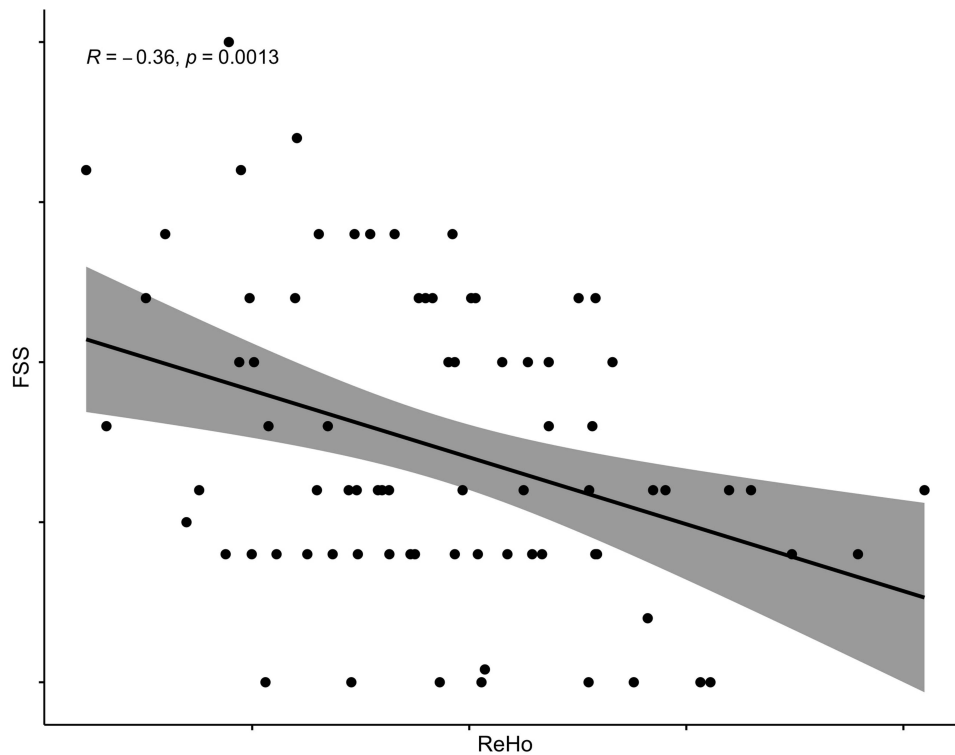


Figure 3 The ReHo values in the precentral and postcentral gyri were negatively correlated with the FSS ($r = -0.36$, $p = 0.0013$).

Abbreviations: ReHo, regional homogeneity; FSS, fatigue severity score.

As opposed to the brain functional indices pertinent to long-range connectivity such as functional connectivity and degree centrality, fALFF and ReHo are voxel-based metrics indicative of spontaneous neural activities in spatially discrete regions.²⁶ While fALFF estimates the contribution of low-frequency fluctuations to the whole power spectrum,¹¹ ReHo reflects the local synchronization of band-filtered BOLD signals with the neighboring voxels.¹⁷ It has been well established that there is a positive correlation between fALFF and ReHo values.²⁷ More importantly, fALFF and ReHo values exhibited significant correspondence with hemodynamic and metabolic variables acquired from positron emission tomography scans, reflective of underlying metabolic demand.²⁸ In the current study, the significant overlapping areas between fALFF and ReHo maps further substantiated the correspondence between these two metrics, since both fALFF and ReHo analysis consistently revealed elevated activity at the bilateral precentral and postcentral gyrus, bilateral middle occipital gyrus and the left insular cortex, as well as decreased activity at the bilateral posterior lobe of cerebellum. In addition to the measures of local spontaneous neural activities, emerging evidence shows that diseases could be better anchored to distributed brain networks than discrete anatomical brain regions, with multiple recent efforts to examine the functional connectivity network mapping (FCNM) in different diseases.^{29,30} We also intend to examine the findings of the current study from the perspective of brain network localization in the future.

Two earlier studies examined the ALFF or the low-frequency oscillations (LFOs) in AS patients, revealing extensive alterations of spontaneous neural activities through the analysis of low-frequency fluctuations.^{14,15} In contrast to ALFF, in this study we adopted fALFF, which is more robust and less susceptible to motion artifacts as well as physiological noise.^{11,12} Consistent with the earlier reports, key nodes of the triple network model exhibited significant alterations, including the MTG, precuneus and mPFC from the DMN, the insular cortex and the ACC from the SN, and the dlPFC from the FPN. An intriguing observation is that the dorsal elements of the triple network model generally exhibited elevated fALFF and ReHo values, such as the PCC/precuneus and MTG, whereas the ventral elements generally exhibited decreased fALFF and ReHo values, such as the mPFC, ACC, and dlPFC. In the LFOs study by Rogachov et al, AS patients also exhibited increased LFOs in the PCC/PCu and MCC of the DMN and SN in the slow-4 band.¹⁵ Similar to our results, Li et al also reported significantly increased ALFF located at the right PCu, left MTG, both belonging to the dorsal DMN, while the left medial frontal gyrus presented aberrantly decreased ALFF.¹⁴ It was proposed that aberrations of the triple network model significantly contributed to multiple psychiatric and neurological disorders, including schizophrenia,³¹ compulsory obsessive disorder³² and fibromyalgia.³³ DMN is an integrated network system responsible for multiple aspects of self-referential mental activities, whereas FPN is an external-oriented network responsible for goal-directed behavior, such as working memory, decision making, direction of attention, and planning.³⁴ The salience network is a fast-acting hub responsible for salience detection, thereby facilitating the switch between DMN and FPN.³⁵ Previous studies utilizing SCA,^{8,36} ICA³⁶ and graph-theory-based analysis⁹ consistently reported the aberrations within this triple network model, notably the disruptions of the anti-correlation between SN, FPN and DMN, indicating diminished capability to divert cognitive resources from self-referential mental activities to external-oriented behavior. In the current study, we found that there was an imbalance in fALFF and ReHo values between the dorsal and ventral elements of the triple network, showing that not only was the global integration of the triple network model disrupted, but the local spontaneous neural activities within each network were also altered.

Notably, the bilateral dlPFC in the FPN exhibited significantly decreased ReHo values in this study. It has been established that the dlPFC functions as the hub responsible for the cognitive reappraisal and modulation of pain experience.^{37,38} One study revealed that decreased activation of the dlPFC was associated with poor coping in the expectation of pain in patients with fibromyalgia and osteoarthritis,³⁹ while another study also showed that in patients with fibromyalgia, the resting-state functional connectivity between the dlPFC and rostral ACC as well as the mPFC could be significantly increased following effective treatment.⁴⁰ Our results showed that the spontaneous neural activities at the dlPFC were significantly decreased in AS patients, indicating that the cognitive resources fail to be reallocated to this pain reappraisal and modulation hub, thereby causing heightened pain experiences.

Another interesting finding of this study is that both fALFF and ReHo analyses revealed significantly increased spontaneous neural activities in the bilateral precentral and postcentral gyri, both belonging in the sensorimotor network. While the precentral gyrus is responsible for controlling the voluntary motor movement,⁴¹ the postcentral gyrus receives afferent sensational stimuli and perceives sensations.^{42,43} Li et al reported that the ALFF in the left postcentral gyrus was increased, while the right precentral gyrus exhibited decreased ALFF on the contrary.¹⁴ This discrepancy could be attributed to the methodology (ALFF vs fALFF) as well as the different sizes of the study samples, as Li et al only recruited 27 AS patients. The alterations of the sensorimotor network in AS patients could be explained by the musculoskeletal pain caused by inflammation of the axial skeleton or peripheral joints, as well as its impact on movement. Interestingly, the results of the correlation analysis showed a negative correlation between the ReHo values of this area and FSS, which is a scale quantifying the severity of fatigue. Moreover, our study also consistently showed increased fALFF and ReHo values in the bilateral cuneus, which forms part of the visual cortex and is considered the core architecture for the integration of visual information.⁴⁴ A previous study employing graph theory analysis also reported nodal changes in the visual network in AS patients.⁹ It was proposed that this alteration might be an adaptive neural remodeling process, and that AS patients could facilitate the adjustments of position or movement with the input from the visual system.^{9,45}

Although the cerebellum was previously not considered a structure pertinent to pain perception, accumulating evidence suggests that the cerebellum is also implicated in the processing of pain, especially lobules IV–VI and Crus I and II.^{46,47} It has been established that the cerebellum plays a significant role in inhibiting pain perception with Crus I, Crus II and lobule VI, with potential involvements in pain anticipation, perception and the emotional aspects of pain.⁴⁸ One study used arterial spin labeling to demonstrate that chronic neuropathic pain was associated with decreased blood flow in lobules V and VI.⁴⁹ Moreover, meta-analyses of pain neuroimaging studies also showed altered activation in lobules V, VI, and Crus I in conditions of chronic pain.^{50,51} Voxel-based morphometric studies on fibromyalgia also consistently exhibited significantly decreased gray matter volume in the posterior lobe of the cerebellum.^{52–54} In the current study, we found that the fALFF and ReHo values were consistently decreased in the posterior lobe of the cerebellum, while the ReHo values at the anterior lobe of the cerebellum were increased. Li et al also reported increased ALFF values in the anterior lobe of the cerebellum.¹⁴ Given the importance of the posterior lobe of cerebellum in pain inhibition, the consistently decreased fALFF and ReHo could indicate diminished ability of pain modification. However, we could not establish an association between cerebellar activation and pain severity in the correlation analysis. Whether the aberrant cerebellar activation in AS patients is associated with pain perception requires further investigation.

In this study, we also examined the contribution of the slow-5 and slow-4 bands to the fALFF of the standard frequency band. Results showed that while slow-5 and slow-4 both contributed to the significantly decreased fALFF values in the posterior lobe of the cerebellum, only slow-4 contributed to all the elevated fALFF values in the standard frequency band. In the slow-5 band analysis, all three clusters showed significantly decreased fALFF values. Little is known about the neurobiological mechanisms underlying the different frequency bands of fALFF, but it was reported that the rhythmic depolarization-hyperpolarization sequence generated by the excitatory and inhibitory postsynaptic potentials (PSP) could be involved in the low-frequency oscillations.⁵⁵ Moreover, non-neuronal cells such as astrocytes could be involved in the regulation and maintenance of LFOs.^{12,16} Previous studies have shown that both slow-5 and slow-4 oscillations were primarily detected within gray matter, as opposed to slow-3 and slow-2 oscillations, which were restricted to white matter.¹² Sub-band analysis of ALFF or fALFF have been conducted in multiple psychiatric and neurological disorders, such as bipolar II depression,⁵⁶ insomnia⁵⁷ and hypothyroidism,⁵⁸ and accumulating evidence suggests that the sub-band differences could be more sensitive to the frequency-specific alterations in discrete spatial locations.^{58,59} Rogachov et al showed that AS patients had increased LFOs within the ascending pain pathway including thalamus and S1 in both slow-5 and slow-4 bands, indicating the continuous yet fluctuating sensory input of chronic pain, while in the slow-4 band, LFOs were also increased in the posterior cingulate cortex and middle cingulate cortex of the DMN and SN, which could be explained by the pain-related rumination and negatively valenced internal thoughts.¹⁵ Alshelhi et al also reported that the increased LFOs within the ascending pain pathway was restricted to 0.04Hz (slow-5 to slow-4 border) in

neuropathic pain patients.¹⁶ Although we did not find alterations of the slow-5 band fALFF in the thalamus in the current study, we showed that the fALFF values were significantly increased within the sensori-motor network, including S1, in the slow-4 band instead of the slow-5 band, contrary to the study by Rogachov et al.¹⁵ This finding could be construed as significantly heightened, fluctuating nociceptive input resulting from the chronic pain experienced by the AS patients, which was transmitted at a higher frequency. On the other hand, the fALFF values were significantly decreased within the posterior lobe of the cerebellum across the slow-5 band and the slow-4 band, indicating diminished ability of pain modification,¹² which was significant in different frequency bands. The differential contribution of the slow-5 and slow-4 bands indicated that the slow-4 band might be more sensitive to the elevated fALFF values in AS patients than the slow-5 band, while the significant alterations, notably in the posterior lobe of the cerebellum, could be detected by both slow-4 and slow-5 bands. More in-depth mechanistic research is warranted to fully understand the neuropathophysiological significance of the different frequency bands of fALFF.

There are several limitations to this study. First, since this was a cross-sectional study, we could not establish a causal relationship between the alterations of the local spontaneous neural activities and the disease. It remains unclear whether the alterations of fALFF and ReHo reflect trait-like adaptations innate to the disease per se or state-dependent changes that could be restored once the inflammation is resolved. Longitudinal studies are required to verify whether remission of active disease can restore the fALFF and ReHo alterations. In addition, modulation analysis could be conducted to reveal the modulation effects of disease activity and current pain status on neural activities. Second, despite our efforts to minimize the potential impact of medication on fALFF and ReHo by excluding patients currently on bDMARDs, other medications such as NSAIDs could still potentially influence the local neural activities. However, it was reported that NSAIDs such as celecoxib did not affect the resting-state functional connectivity in patients with knee osteoarthritis, since NSAIDs mainly achieve pain relief primarily through local anti-inflammatory mechanism, while its impact on the supraspinal level is minimal.

Conclusion

In conclusion, both fALFF and ReHo analyses consistently exhibited extensive alterations of local spontaneous neural activities in brain regions belonging to the DMN, SN, FPN, sensorimotor network, visual network and the cerebellum. This study provides further evidence that aberrations of the triple network model serve as an important feature of AS from the perspective of local neural activities. Compared with the slow-5 frequency band, slow-4 was the major contributor to the elevated low-frequency fluctuations, whereas analysis of the slow-5 band mostly showed decreased fALFF values. These results deepen our understanding of the neuropathophysiological mechanisms underlying the pain perception in AS.

Funding

This work was supported by the grants from Guangdong Clinical Research Center of Immune Disease (2020B111170008); Key-Area Research and Development Program of Guangdong Province (2023B1111030002); Guangdong Provincial Medical Science and Technology Research Fund (A2024531); Guangdong Provincial Medical Science and Technology Research Fund (A2024574); Science and Technology Projects in Guangzhou (2023A04J1092); Hospital National Natural Science Foundation Cultivation Project (2021GZRPYM06); Five-Five Project of the Third Affiliated Hospital of Sun Yat-sen University (2023WW605).

Disclosure

Churong Lin and Ya Xie are co-first authors for this study. The authors report no conflicts of interest in this work.

References

1. Robinson PC, van der Linden S, Khan MA, Taylor WJ. Axial spondyloarthritis: concept, construct, classification and implications for therapy. *Nat Rev Rheumatol.* 2021;17(2):109–118. doi:10.1038/s41584-020-00552-4

2. Taurog JD, Chhabra A, Colbert RA. Ankylosing spondylitis and axial spondyloarthritis. *N Engl J Med.* 2016;374(26):2563–2574. doi:10.1056/NEJMra1406182
3. Sieper J, Poddubnyy D. Axial spondyloarthritis. *Lancet.* 2017;390(10089):73–84. doi:10.1016/S0140-6736(16)31591-4
4. Pathan EMI, Inman RD. Pain in axial spondyloarthritis: insights from immunology and brain imaging. *Rheum Dis Clin North Am.* 2021;47(2):197–213. doi:10.1016/j.rdc.2020.12.007
5. Guler MA, Celik OF, Ayhan FF. The important role of central sensitization in chronic musculoskeletal pain seen in different rheumatic diseases. *Clin Rheumatol.* 2020;39(1):269–274. doi:10.1007/s10067-019-04749-1
6. Wu Q, Inman RD, Davis KD. Neuropathic pain in ankylosing spondylitis: a psychophysics and brain imaging study. *Arthritis Rheum.* 2013;65(6):1494–1503. doi:10.1002/art.37920
7. Raimondo L, Láf O, Heij J, et al. Advances in resting state fMRI acquisitions for functional connectomics. *NeuroImage.* 2021;243.
8. Hemington KS, Wu Q, Kucyi A, Inman RD, Davis KD. Abnormal cross-network functional connectivity in chronic pain and its association with clinical symptoms. *Brain Struct Funct.* 2016;221(8):4203–4219. doi:10.1007/s00429-015-1161-1
9. Liu Q, Liao Z, Zhang Y, et al. Pain- and fatigue-related functional and structural changes in ankylosing spondylitis: an fMRI study. *Front Med.* 2020;7:193. doi:10.3389/fmed.2020.00193
10. Liu D, Zhang Y, Zhao J, et al. Alterations of the resting-state brain network connectivity and gray matter volume in patients with fibromyalgia in comparison to ankylosing spondylitis. *Scientific Reports.* 2024;14(1).
11. Zou Q-H, Zhu C-Z, Yang Y, et al. An improved approach to detection of amplitude of low-frequency fluctuation (ALFF) for resting-state fMRI: fractional ALFF. *Journal of Neuroscience Methods.* 2008;172(1):137–141. doi:10.1016/j.jneumeth.2008.04.012
12. Zuo X-N, Di Martino A, Kelly C, et al. The oscillating brain: complex and reliable. *NeuroImage.* 2010;49(2):1432–1445. doi:10.1016/j.neuroimage.2009.09.037
13. Buzsáki G, Draguhn A. Neuronal oscillations in cortical networks. *Science.* 2004;304(5679):1926–1929. doi:10.1126/science.1099745
14. Li C, Wei X, Zou Q, et al. Cerebral functional deficits in patients with ankylosing spondylitis- an fMRI study. *Brain Imaging and Behavior.* 2016;11(4):936–942. doi:10.1007/s11682-016-9565-y
15. Rogachov A, Cheng JC, Hemington KS, et al. Abnormal low-frequency oscillations reflect trait-like pain ratings in chronic pain patients revealed through a machine learning approach. *The Journal of Neuroscience.* 2018;38(33):7293–7302. doi:10.1523/JNEUROSCI.0578-18.2018
16. Alshelh Z, Di Pietro F, Youssef AM, et al. Chronic neuropathic pain: it’s about the rhythm. *The Journal of Neuroscience.* 2016;36(3):1008–1018. doi:10.1523/JNEUROSCI.2768-15.2016
17. Zang Y, Jiang T, Lu Y, He Y, Tian L. Regional homogeneity approach to fMRI data analysis. *NeuroImage.* 2004;22(1):394–400. doi:10.1016/j.neuroimage.2003.12.030
18. Linden SVD, Valkenburg HA, Cats A. Evaluation of diagnostic criteria for ankylosing spondylitis. *Arthritis & Rheumatism.* 2005;27(4):361–368. doi:10.1002/art.1780270401
19. Krupp LB. The fatigue severity scale. *Archives of Neurology.* 1989;46(10):1121. doi:10.1001/archneur.1989.00520460115022
20. Zochling J. Measures of symptoms and disease status in ankylosing spondylitis: ankylosing Spondylitis Disease Activity Score (ASDAS), Ankylosing Spondylitis Quality of Life Scale (ASQoL), Bath Ankylosing Spondylitis Disease Activity Index (BASDAI), Bath Ankylosing Spondylitis Functional Index (BASFI), Bath Ankylosing Spondylitis Global Score (BAS-G), Bath Ankylosing Spondylitis Metrology Index (BASMI), Dougados Functional Index (DFI), and Health Assessment Questionnaire for the Spondylarthropathies (HAQ-S). *Arthritis Care & Research.* 2011;63:S11.
21. Yan C-G, Wang X-D, Zuo X-N, Zang Y-F. DPABI: data Processing & Analysis for (Resting-State) Brain Imaging. *Neuroinformatics.* 2016;14(3):339–351. doi:10.1007/s12021-016-9299-4
22. Friston KJ, Williams S, Howard R, Frackowiak RSJ, Turner R. Movement-Related effects in fMRI time-series. *Magnetic Resonance in Medicine.* 2011;35(3):346–355. doi:10.1002/mrm.1910350312
23. Jenkinson M, Bannister P, Brady M, Smith S. Improved optimization for the robust and accurate linear registration and motion correction of brain images. *NeuroImage.* 2002;17(2):825–841. doi:10.1006/nimg.2002.1132
24. Yan C-G, Zang Y-F. DPARSF: a MATLAB toolbox for “pipeline” data analysis of resting-state fMRI. *Frontiers in System Neuroscience.* 2010. doi:10.3389/fnsys.2010.00013
25. Menon V. Large-scale brain networks and psychopathology: a unifying triple network model. *Trends Cogn Sci.* 2011;15(10):483–506. doi:10.1016/j.tics.2011.08.003
26. Zhao L, Bo Q, Zhang Z, Li F, Zhou Y, Wang C. Disrupted default mode network connectivity in bipolar disorder: a resting-state fMRI study. *BMC Psychiatry.* 2024;24(1). doi:10.1186/s12888-024-05869-y
27. Yan CG, Yang Z, Colcombe SJ, Zuo X-N, Milham MP. Concordance among indices of intrinsic brain function: insights from inter-individual variation and temporal dynamics. *Science Bulletin.* 2017;62(23):1572–1584. doi:10.1016/j.scib.2017.09.015
28. Deng S, Franklin CG, O’Boyle M, et al. Hemodynamic and metabolic correspondence of resting-state voxel-based physiological metrics in healthy adults. *NeuroImage.* 2022;250.
29. Mo F, Zhao H, Li Y, et al. Network localization of state and trait of auditory verbal hallucinations in schizophrenia. *Schizophrenia Bulletin.* 2024;50(6):1326–1336. doi:10.1093/schbul/sbae020
30. Cheng Y, Cai H, Liu S, et al. Brain network localization of gray matter atrophy and neurocognitive and social cognitive dysfunction in schizophrenia. *Biological Psychiatry.* 2025;97(2):148–156. doi:10.1016/j.biopsych.2024.07.021
31. Stephan KE, Friston KJ, Frith CD. Dysconnection in schizophrenia: from abnormal synaptic plasticity to failures of self-monitoring. *Schizophr Bull.* 2009;35(3):509–527. doi:10.1093/schbul/sbn176
32. Gursel DA, Reinholz L, Bremer B, et al. Frontoparietal and salience network alterations in obsessive-compulsive disorder: insights from independent component and sliding time window analyses. *J Psychiatry Neurosci.* 2020;45(3):214–221. doi:10.1503/jpn.190038
33. Cifre I, Sitges C, Fraiman D, et al. Disrupted functional connectivity of the pain network in fibromyalgia. *Psychosom Med.* 2012;74(1):55–62. doi:10.1097/PSY.0b013e3182408f04
34. Menon V, D’Esposito M. The role of PFC networks in cognitive control and executive function. *Neuropsychopharmacology.* 2022;47(1):90–103. doi:10.1038/s41386-021-01152-w

35. Menon V, Uddin LQ. Saliency, switching, attention and control: a network model of insula function. *Brain Structure and Function*. 2010;214(5-6):655–667. doi:10.1007/s00429-010-0262-0
36. Liu D, Lin C, Liu B, et al. Resting-state functional connectivity between the frontoparietal network and the default mode network is aberrantly increased in ankylosing spondylitis. *BMC Musculoskeletal Disorders*. 2025;26(1).
37. Lorenz J, Minoshima S, Casey KL. Keeping pain out of mind: the role of the dorsolateral prefrontal cortex in pain modulation. *Brain*. 2003;126(5):1079–1091. doi:10.1093/brain/awg102
38. Seminowicz DA, Moayedi M. The dorsolateral prefrontal cortex in acute and chronic pain. *The Journal of Pain*. 2017;18(9):1027–1035. doi:10.1016/j.jpain.2017.03.008
39. Brown CA, El-Deredy W, Jones AK. When the brain expects pain: common neural responses to pain anticipation are related to clinical pain and distress in fibromyalgia and osteoarthritis. *Eur J Neurosci*. 2014;39(4):663–672. doi:10.1111/ejn.12420
40. Kong J, Wolcott E, Wang Z, et al. Altered resting state functional connectivity of the cognitive control network in fibromyalgia and the modulation effect of mind-body intervention. *Brain Imaging Behav*. 2018;13(2):482–492.
41. Chouinard PA, Paus T. The primary motor and premotor areas of the human cerebral cortex. *The Neuroscientist*. 2006;12(2):143–152. doi:10.1177/1073858405284255
42. Feldman DE, Brecht M. map plasticity in somatosensory cortex. *Science*. 2005;310(5749):810–815. doi:10.1126/science.1115807
43. Velasques B, Machado S, Paes F, et al. Sensorimotor integration and psychopathology: motor control abnormalities related to psychiatric disorders. *World J Bio Psychiatry*. 2011;12(8):560–573. doi:10.3109/15622975.2010.551405
44. Tomasi D, Volkow ND. Association between functional connectivity hubs and brain networks. *Cerebral Cortex*. 2011;21(9):2003–2013. doi:10.1093/cercor/bhq268
45. Pomper U, Höfle M, Hauck M, Kathmann N, Engel AK, Senkowski D. Crossmodal bias of visual input on pain perception and pain-induced beta activity. *NeuroImage*. 2013;66:469–478. doi:10.1016/j.neuroimage.2012.10.040
46. Moulton EA, Schmahmann JD, Becerra L, Borsook D. The cerebellum and pain: passive integrator or active participator? *Brain Research Reviews*. 2010;65(1):14–27. doi:10.1016/j.brainresrev.2010.05.005
47. Li CN, Keay KA, Henderson LA, Mychasiuk R. Re-examining the mysterious role of the cerebellum in pain. *J Neurosci*. 2024;44(17). doi:10.1523/JNEUROSCI.1538-23.2024
48. Manda O, Hadjivassiliou M, Varrassi G, Zavridis P, Zis P. Exploring the role of the cerebellum in pain perception: a narrative review. *Pain and Therapy*. 2025;14(3):803–816. doi:10.1007/s40122-025-00724-8
49. Youssef AM, Gustin SM, Nash PG, et al. Differential brain activity in subjects with painful trigeminal neuropathy and painful temporomandibular disorder. *Pain*. 2014;155(3):467–475. doi:10.1016/j.pain.2013.11.008
50. Jensen KB, Regenbogen C, Ohse MC, Frasnelli J, Freiherr J, Lundström JN. Brain activations during pain. *Pain*. 2016;157(6):1279–1286. doi:10.1097/j.pain.0000000000000517
51. Xu A, Larsen B, Henn A, et al. Brain responses to noxious stimuli in patients with chronic pain. *JAMA Network Open*. 2021;4(1):e2032236. doi:10.1001/jamanetworkopen.2020.32236
52. Schmidt-Wilcke T, Luerding R, Weigand T, et al. Striatal grey matter increase in patients suffering from fibromyalgia—a voxel-based morphometry study. *Pain*. 2007;132 Suppl 1:S109-S16.
53. Mosch B, Hagen V, Herpertz S, Diers M. Brain morphometric changes in fibromyalgia and the impact of psychometric and clinical factors: a volumetric and diffusion-tensor imaging study. *Arthritis Res Ther*. 2023;25(1):81. doi:10.1186/s13075-023-03064-0
54. Shi H, Yuan C, Dai Z, Ma H, Sheng L. Gray matter abnormalities associated with fibromyalgia: a meta-analysis of voxel-based morphometric studies. *Semin Arthritis Rheum*. 2016;46(3):330–337. doi:10.1016/j.semarthrit.2016.06.002
55. Steriade M, Nunez A, Amzica F. A novel slow (< 1 Hz) oscillation of neocortical neurons in vivo: depolarizing and hyperpolarizing components. *The Journal of Neuroscience*. 1993;13(8):3252–3265. doi:10.1523/JNEUROSCI.13-08-03252.1993
56. Zhou J, Ma X, Li C, et al. Frequency-specific changes in the fractional amplitude of the low-frequency fluctuations in the default mode network in medication-free patients with bipolar ii depression: a longitudinal functional MRI study. *Frontiers in Psychiatry*. 2021;11.
57. Zhou F, Huang S, Zhuang Y, Gao L, Gong H. Frequency-dependent changes in local intrinsic oscillations in chronic primary insomnia: a study of the amplitude of low-frequency fluctuations in the resting state. *NeuroImage: Clinical*. 2017;15:458–465. doi:10.1016/j.nicl.2016.05.011
58. Zhao L, Cao J, Qin R, et al. Frequency-specific alterations of fractional amplitude of low-frequency fluctuations in adult-onset hypothyroidism. *Journal of Integrative Neuroscience*. 2024;23(6).
59. Han Y, Wang J, Zhao Z, et al. Frequency-dependent changes in the amplitude of low-frequency fluctuations in amnesic mild cognitive impairment: a resting-state fMRI study. *NeuroImage*. 2011;55(1):287–295. doi:10.1016/j.neuroimage.2010.11.059